



ISSN 1823-626X

Malaysian Journal of Fundamental and Applied Sciences

 available online at <http://mjfas.ibnusina.utm.my>


Conductivity and Dielectric Behaviour Studies of LiCF₃SO₃ Dissociation in L-Chitosan/PMMA-Based Polymer Electrolytes

A.S.A Khiar*, S. Mat Radzi and N. Abd Razak

Faculty of Science and Technology, Universiti Sains Islam Malaysia, Bandar Baru Nilai, 71800 Nilai, Negeri Sembilan, Malaysia

Received 20 November 2012, Revised 19 February 2013, Accepted 22 February 2013, Available online 26 February 2013

ABSTRACT

Lauroyl-chitosan/poly(methylmethacrylate)-lithium trifluorosulfonate (LiCF₃SO₃) polymer electrolytes has been prepared by the solution casting method. Ionic conductivity analysis was conducted over a wide range of frequency between 50 Hz-1 MHz using impedance spectroscopy to evaluate the dielectric properties and conductivity of the sample. Sample with 30 wt% of LiCF₃SO₃ showed the highest conductivity of $7.59 \pm 3.64 \times 10^{-4} \text{ Scm}^{-1}$ at room temperature. Complex permittivity for real (ϵ_r'), imaginary (ϵ_r'') and electrical modulus for real (M_r') and imaginary (M_r'') part was determined and plotted. The relaxation time, τ for these samples was determined and the plot shows that τ decreases with conductivity of the complexes.

| L-chitosan | PMMA | conductivity | dielectric | polymer electrolytes |

 © 2013 Ibnu Sina Institute. All rights reserved.
<http://dx.doi.org/10.11113/mjfas.v9n1.81>

1. INTRODUCTION

Solid polymer electrolytes based on blending polymer has emerged as an important ionic conductor [1] especially those made from natural polymer. Natural polymers are the most promising biodegradable and biocompatibility materials because it is renewability, readily available, cheap and have good physical and chemical properties [2]. Previous report [3], have shown that although poly(ethylene oxide) gives good performances application as solid polymer electrolyte (SPE), it has limited ionic conductivity at room temperature. Therefore, many researches are doing their best to overcome this disadvantage by finding alternatives for the development of novel SPEs [3].

Chitosan is a natural biopolymer and abundant types polysaccharides derived from chitin of crustaceans such as the crab, crayfish, shrimps, etc. [4,5]. Chitosan structure composed of N-acetylglucosamine (GlcNAc) and glucosamine (GlcN) residues [6]. The repeating unit [β -(1-4) linked 2-amino-2-deoxy-D-glucopyranose] [7] in this polymer consists of one primary hydroxyl groups at C-6 and one secondary hydroxyl groups at C-3 and highly reactive amino groups at C-2 [4] which have lone pair electron that makes it suitable in wide application.

However, the applications of chitosan were limited due to the presence of strong intra and intermolecular hydrogen bond [8,9] from the primary amino groups residues which resulted in the formation of linear aggregates with extensive crystallinity [7].

This rigid crystalline structure makes chitosan poor

in processability and insoluble in water and organic solvent [8,9]. Therefore, in order to improve its ability, acyl modification of chitosan was carried out in the present study [10]. The presences of lone pair electron in the structure of acylated chitosan such as lauroyl (L)-chitosan allowed complexation with the salt. Since L-chitosan is a sticky-type elastic film [10], it would have to be blended with other polymer in order to increase its mechanical stability which is required for solid polymer electrolytes application. In the present study, L-chitosan was blended with poly(methylmethacrylate) (PMMA). PMMA is one of the host polymers previously used in the plasticized polymer electrolyte, which was first reported by Iijima and co-workers [11]. To the best of the author's knowledge, there is no study reported on L-chitosan/PMMA solid polymer electrolytes. Therefore in an attempt to look for a better lithium ion conducting polymer electrolytes, polymer electrolytes based on PMMA/L-Chitosan blend by varying lithium salt concentration is investigated and their characterizations will be discussed in this present paper.

2. EXPERIMENTAL

2.1 Materials and methods

Chitosan flake and PMMA with high molecular weight purchased from Sigma were used without further purification. Pyridine and tetrahydrofuran (THF) purchased from F.S Chemical with purity of 99.5% were used as solvents. Lauroyl Chloride (97.5%, Fluka) was used as the

*Corresponding author. E-mail: azwanisofia@usim.edu.my
 (A.S.A Khiar) Tel : 06-7986507, Fax : 06-7986566.

reacting agent. LiCF_3SO_3 with purity over 96% obtained from Sigma was used as a doping salt for SPE preparation.

2.2 Sample preparations

L-chitosan was prepared initially using method found elsewhere [10]. The appropriate amounts of L-chitosan/PMMA blends have been prepared by mixing both materials with THF. Prior to the preparation of SPE, LiCF_3SO_3 was added into the homogenous solution of L-Chitosan/PMMA with desired amount and stirred continuously for several days. Various compositions of the films are tabulated in Table 1. The homogenous and viscous solution obtained were cast in Teflon petri dishes and allowed to evaporate slowly at room temperature for several days. The free standing films obtained were kept in a drying cabinet for continuous drying before further analysis.

Table 1. Various composition of L-Chitosan and PMMA

Designation	L-Chitosan (wt %)	PMMA (wt %)
PLC0	100	0
PLC1	0	100
PLC2	10	90
PLC3	20	80
PLC4	30	70
PLC5	40	60
PLC6	50	50
PLC7	60	40

2.3 Sample characterization

2.3.1 X-Ray Diffraction

The amorphous structure of the blended L-chitosan/PMMA film with various compositions was investigated using XRD. The XRD pattern were recorded and scanned with a beam of monochromatic $\text{CuK}\alpha$ -X-radiation of wavelength $\lambda = 1.5406\text{\AA}$ over the range of $2\theta = 5^\circ - 80^\circ$.

2.3.2 Conductivity Measurement

Conductivity measurement was carried out using the impedance spectroscopy model HIOKI 3532-50 LCR HiTESTER interfaced to a computer. The thin film in which thickness was measured by using a digital micrometer screw gauge was sandwiched between two electrodes of a sample holder with diameter 1.082 cm, under spring pressure. The data was taken over frequency ranges from 50 Hz to 1 MHz at room temperature. From the data obtained, negative imaginary part of the impedance (Z_i) was plotted versus positive impedance (Z_r). Bulk resistance (R_b)

from intercept at Z_r axis was determined and the conductivity was calculated using equation:

$$\sigma = \frac{t}{R_b A} \quad (1)$$

where R_b represent the bulk resistance, A is the effective area of contact of the sample and t is the thickness of the film. Other recorded data besides impedance $Z(\omega)$, used in impedance spectroscopy are complex permittivity $\epsilon(\omega)$ and complex dielectric modulus $M(\omega)$. Both the real ϵ_r and imaginary part ϵ_i of dielectric constant and electrical modulus as well as loss tangent ($\tan \delta$) can be obtained from the following equations:

$$\epsilon_r(\omega) = \frac{Z_i}{\omega C_0 (Z_r^2 + Z_i^2)} \quad (2)$$

$$\epsilon_i(\omega) = \frac{Z_r}{\omega C_0 (Z_r^2 + Z_i^2)} \quad (3)$$

$$M_r(\omega) = \frac{\epsilon_r}{(\epsilon_r^2 + \epsilon_i^2)} \quad (4)$$

$$M_i(\omega) = \frac{\epsilon_i}{(\epsilon_r^2 + \epsilon_i^2)} \quad (5)$$

$$\tan \delta = \frac{\epsilon_i}{\epsilon_r} \quad (6)$$

where $C_0 = \epsilon_0 A/t$ and ϵ_0 is the permittivity of the free space.

3. RESULTS & DISCUSSION

3.1 X-Ray Diffraction

Fig. 1(a) illustrates the XRD pattern of pure L-chitosan film. The XRD spectrum show a broad reflection centered at $2\theta = 20^\circ$ together with that of strong reflection at $2\theta = 2-5^\circ$. Similar results have been reported by Winie and co workers [12] who studied on the structure of hexanoyl chitosan based polymer electrolytes. Meanwhile, Fig. 1(b) shows the spectrum of pure PMMA that exhibited a semicrystalline feature which is characterized by two halo diffraction pattern centered at $2\theta = 17.7^\circ$ and $2\theta = 31.5^\circ$. This is consistent with that reported by Baskaran and co-workers [13] as well as Rajendran and co-workers [14]. Fig. 1(c-h) illustrate the XRD pattern of L-Chitosan/PMMA blends at different weight percentages. It may be seen that the peaks of L-Chitosan/PMMA blend sample with higher weight percent of PMMA became more intense and a new crystalline peak at $2\theta = 21.4^\circ$ was observed. The blending compositions of 40:60 L-Chitosan/PMMA which has amorphous nature seen from the diffractogram was chosen in the preparation of SPE. The amorphous nature of the polymer structure will causes

a reduction in the energy barrier to the segmental motion of the polymer electrolytes [13].

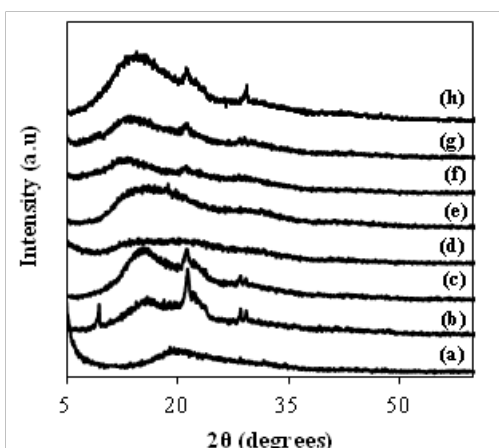


Fig. 1. XRD Diffraction pattern of samples (a) PLC0 (b) PLC1 (c) PLC2 (d) PLC3 (e) PLC4 (f) PLC5 (g) PLC6 and (h) PLC7

3.1 Conductivity and dielectric studies.

Electrical conductivity values at room temperature for L-Chitosan/PMMA with different amounts of LiCF_3SO_3 are shown in Fig. 2. It can be seen that the electrical conductivity value increases with addition of 10-30 wt% salt from which after it decreases. This is due to the number of ion of solvated salt become crowded thus reduces the number of charge carrier [15]. The highest conductivity obtained at the room temperature in the present study is $7.59 \pm 3.64 \times 10^{-4} \text{ Scm}^{-1}$. The increase in conductivity could be due to the increase in the number density of free ions due to dissociation of salt that occurs in the polymer matrix [16], while the decrease in conductivity could be due to the reassociation of ions to form cluster of ions in the polymer-salt system and could also be attributed to the increase in viscosity of the polymer solution [6] prior to formation of the SPE film.

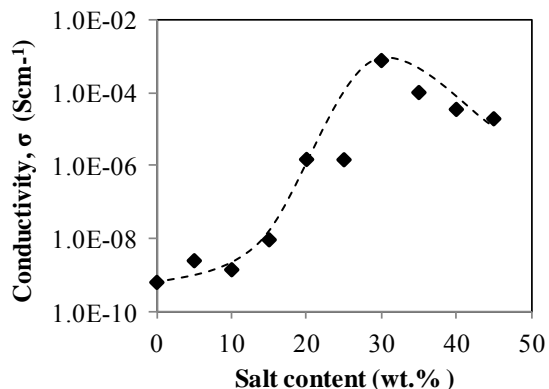


Fig. 2. Room temperature conductivity as a function of salt concentration

Dielectric behaviour studies refer to the behaviour of dielectric relaxation response of dielectric medium to an external electric field. The variation of real, ϵ_r and imaginary, ϵ_i parts of the dielectric constant versus frequency for the samples in the present study are shown in Fig. 3 (a-b), respectively. It could be seen from the figure that there are no appreciable relaxation peaks observed thus; the dielectric constant in this present study act as an indicator to show that the increase in conductivity is due to an increase in the number of density of mobile ions. Both real and imaginary part of dielectric shows the same trend at high frequency; they approach a constant value. At higher frequency, the periodic reversal of the electric field occurs so fast resulted in no excess of ion diffusion in the direction of the field. The decrease in the value of real and imaginary part of dielectric constant is due to the decrease in charge accumulation [17].

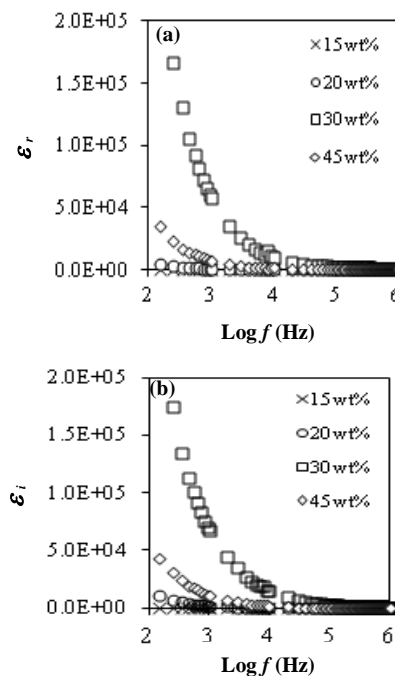


Fig. 3. (a) Real and (b) Imaginary part of dielectric constant as a function of frequency for selected samples

Further analysis of the dielectric behavior can further be confirmed using the formulation of dielectric moduli, which highlights the bulk dielectric behavior and suppresses the effect of electrode polarization. Fig. 4 (a-b) depicts the variations of real and imaginary part of dielectric modulus. The opposite results from the dielectric constant explains the negligible contribution of electrode polarization at low frequencies which is shown from the value approaching zero [18], however definitive dispersion peaks are not observed at higher frequency. In addition, long tails are well present at low frequencies which indicate the large capacitance associated with the electrodes. The curve peaks

at higher frequencies may be attributed to the bulk effect thus indicates that the polymer electrolytes films are ionic conductors [19]. The variation of loss tangent ($\tan \delta$) as a function of frequency for sample containing various LiCF_3SO_3 is shown in Fig. 5. It is clearly observed that loss tangent increases with increasing frequency passing through the maximum value before decreases and this result is consistent with that of the conductivity value. The shift of maximum $\tan \delta$ towards higher frequency explained quicker relaxation time which can be seen for the highest conductivity value peak frequency shifting towards higher frequency side.

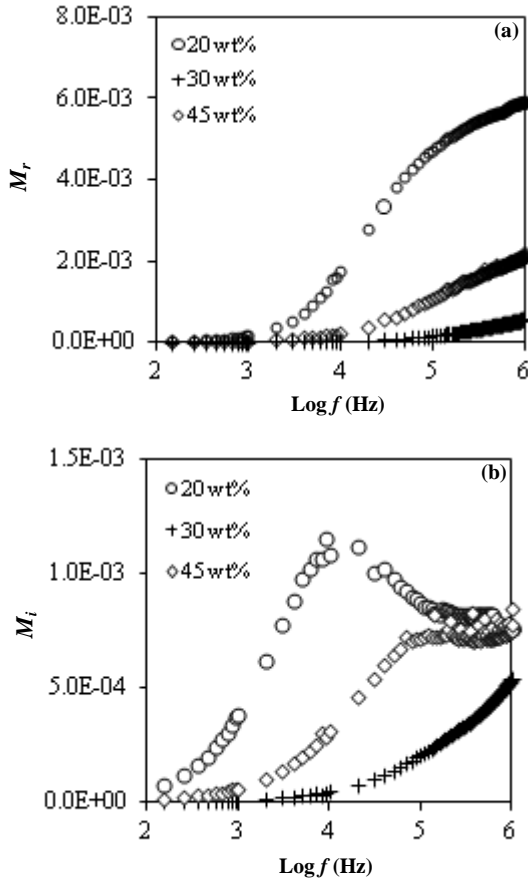


Fig. 4. (a) Real and (b) Imaginary part of dielectric modulus as a function of frequency for selected samples

The occurrence of relaxation time is the result of the efforts carried out by ionic charges carriers within the host polymer material to obey the change in the direction of applied field. This can be defined by the relation:

$$\tau\omega = 1 \tag{8}$$

where τ is the relaxation time, ω is the angular velocity with $\omega=2\pi f$, f is the frequency value corresponding to maximum $\tan \delta$.

The salt concentration dependence of the dielectric constant at selected frequencies is shown in Fig. 6. The graph follows almost the same trend as the conductivity plot shown in Fig. 2. It can be observed that ϵ_r value increases with addition of salt content for every frequency until a maximum addition of 30 wt% of LiCF_3SO_3 from which after it starts to decline. This phenomenon implies that, the number of charge carrier has increased in the sample containing Li^+ ion. Since the dielectric constant refers to the stored charge (which is ions) in the materials, therefore, the increase in charge gives the result of increasing the value of conductivity [20].

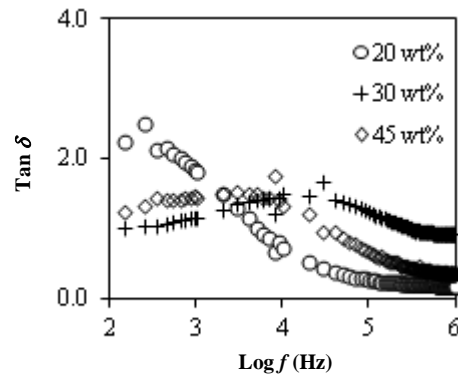


Fig. 5. The variation of loss tangent as a function of frequency for selected samples

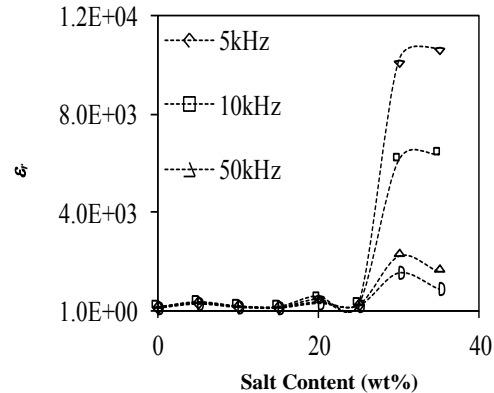


Fig. 6. Salt concentration dependence for selected samples of dielectric constant at selected frequencies

4. CONCLUSION

Lauroyl chitosan were synthesized by acyl modification. The lauroyl chitosan exhibited excellent solubility in common organic solvents and good film forming ability when blended with PMMA. XRD showed the influence of PMMA onto L-Chitosan. The composition of 40:60 blending of L-chitosan and PMMA was selected as the polymer host for SPE preparation. The variation in conductivity with varying salt composition has been analyzed quantitatively.

ACKNOWLEDGEMENT

This work was funded by FRGS under vote USIM/FRGS-FST-06-50208. N.A. Razak would like to thank MOSTI for the scholarship awarded under the National Science Fellowship (NSF) Scheme.

REFERENCES

- [1] R.I Mattos, A. Pawlicka, J.F Lima, C.E Tambelli, C.J. Magon & J.P Donoso, *Electrochim Acta* Vol. 55 (2010), 1396-1400
- [2] D. F Vieira & A. Pawlicka, *Electrochim Acta* 55 (2010), 1489-1494
- [3] W. Ning, Z. Xingxiang, L. Haihui L & W. Jianping, *Carbohydr Polym.* 77 (2009), 607-611
- [4] W. Ying, A.M.C Katherine, P. Brant & B.V. Tam, *J Membrane Sci* Vol. 280, (2006), 666-674
- [5] K.L Jung, U.K. Soo & H.K. Jung, *Biosci Biotech Bioch* 63 (1999), 833-839
- [6] M.F.Z. Kadir, S.R. Majid & A.K. Arof, *Electrochim Acta* 55 (2010), 1475-1482
- [7] K.V. Harish Prashanth & R.N. Tharanathan, *Trends Food Sci Tech* 18 (2007), 117-131
- [8] M. Guiping, Y. Dongzhi, F.K. John & N. Jun, *Carbohydr Polym* Vol.75, (2009), 390-394
- [9] M. Guiping, L. Yang, F.K. John & N. Jun, *Carbohydr Polym* 14 (2011), 681-685
- [10] Z. Zong, Y. Kimura, Takahashi & H. Yamane, *Polymer* 41 (2000), 899-906
- [11] S. Rajendran, T. Uma, *Bull Mater Sci* 23 (2000), 27-29
- [12] T. Winie, S. Ramesh & A.K. Arof, *Physica B* 404 (2009), 4308-4311
- [13] R. Baskaran, S. Selvasekaran, N. Kuwata, J. Kawamura, T. Hattori, *Solid State Ionics* 177 (2006), 2679-2682
- [14] S. Rajendran, O. Mahendran, R. Kannan, J. *Solid State Electrochem* 6 (2002), 560-564
- [15] L.S. Ng & A.A Mohamad, *J. Power Sources* 163 (2006), 382-385
- [16] H.J. Woo, S.R. Majid, A.K. Arof, *Solid State Ionics* 199-200 (2011), 14-20
- [17] S. Ramesh, A.H. Yahaya & A.K. Arof, *Solid State Ionics* 152-153 (2002), 291-294
- [18] A. Bhide & K. Hariharan, *Eur Polym J* Vol.43 (2007), 4253-4270
- [19] S.R. Majid & A.K. Arof, *Physica B* 390 (2007), 209-241
- [20] M.H. Buraidah, L.P Teo, S.R. Majid, A.K. Arof, *Physica B* 404 (2009), 1373-1379